

# Symmetry-Aware Steering of Equivariant Diffusion Policies: Benefits and Limits<sup>★</sup>

Minwoo Park<sup>\*,1</sup> Junwoo Chang<sup>\*,1</sup> Jongeun Choi<sup>\*</sup>  
Roberto Horowitz<sup>\*\*</sup>

<sup>\*</sup> Yonsei University, Seoul 03722, Republic of Korea

<sup>\*\*</sup> University of California, Berkeley, CA 94720, USA

e-mail: {minwoopark, junwoochang, jongeunchoi}@yonsei.ac.kr,  
horowitz@berkeley.edu

---

## Abstract:

Equivariant diffusion policies (EDPs) combine the generative expressivity of diffusion models with the strong generalization and sample efficiency afforded by geometric symmetries. While steering these policies with reinforcement learning (RL) offers a promising mechanism for fine-tuning beyond demonstration data, directly applying standard (non-equivariant) RL can be sample-inefficient and unstable, as it ignores the symmetries that EDPs are designed to exploit. In this paper, we theoretically establish that the diffusion process of an EDP is equivariant, which in turn induces a group-invariant latent-noise MDP that is well-suited for equivariant diffusion steering. Building on this theory, we introduce a principled symmetry-aware steering framework and compare standard, equivariant, and approximately equivariant RL strategies through comprehensive experiments across tasks with varying degrees of symmetry. While we identify the practical boundaries of strict equivariance under symmetry breaking, we show that exploiting symmetry during the steering process yields substantial benefits—enhancing sample efficiency, preventing value divergence, and achieving strong policy improvements even when EDPs are trained from extremely limited demonstrations.

*Keywords:* Robot learning and adaptation, AI-powered robotics, Robotic grasping and manipulation, Reinforcement learning, Geometric deep learning

---

## 1. INTRODUCTION

Leveraging geometric symmetries via group-equivariant networks has emerged as a promising direction for improving sample efficiency and generalization in robot learning (Ryu et al., 2023; Seo et al., 2023; Ryu et al., 2024; Seo et al., 2025a; Van der Pol et al., 2020; Wang et al., 2022a; Seo et al., 2025b). Building on this, **Equivariant Diffusion Policies (EDPs)** (Wang et al., 2024) integrate the generative expressivity of Diffusion Policies (Chi et al., 2023) with the structural efficiency of equivariant architectures. Despite their success, policies trained purely on demonstrations often remain suboptimal and can be further improved through online fine-tuning using reinforcement learning (RL) (Ren et al., 2024). To address the computational challenges associated with fine-tuning, a highly efficient method known as **Diffusion Steering via Reinforcement Learning (DSRL)** (Wagenmaker et al., 2025) has been proposed. Instead of updating the diffusion policy’s weights, DSRL treats the pre-trained model as a black box and trains an RL agent to select an optimal initial latent noise for the denoising process. This approach

circumvents the computational cost of backpropagation through the base policy, while achieving high sample efficiency and significant performance improvements.

However, the effectiveness of DSRL relies on the base policy’s ability to cover the state space, which typically requires training on large-scale expert demonstrations for complex tasks. EDPs offer a compelling solution to this data dependency by generalizing efficiently from small datasets. Therefore, steering EDPs could enable high-performance policies trained with significantly fewer expert demonstrations. Despite this potential, this direction remains unexplored. Furthermore, while a naive application of standard DSRL to EDPs is feasible, it ignores the geometric symmetries exploited by the base EDP, possibly causing sample inefficiency during the steering process.

In this work, we investigate the steering of EDPs to address this limitation. We first theoretically establish that an EDP’s diffusion process is equivariant, which leads to the group-invariance of the induced latent-noise MDP. Grounded on this theory, we propose a principled equivariant steering framework for EDPs. We then investigate the relative efficacy in diffusion steering of standard, equivariant, and approximately-equivariant RL, the latter of which encourages symmetry via soft constraints rather than strict equivariance (Finzi et al., 2021; Wang et al., 2022b; Chang et al., 2025). Through simulation experiments across varying degrees of symmetry, we show the

---

<sup>★</sup> This work was supported by the National Research Foundation of Korea (NRF) grant funded by the Korea government (MSIT) (No.RS-2024-00344732). This work was also supported by the Korea Institute of Science and Technology (KIST) Institutional Program (Project No.2E33801-25-015).

<sup>1</sup> Equally contributed.

substantial benefits of our equivariant steering framework, while identifying the practical boundaries of strict equivariance.

Our main contributions are as follows. First, we provide a theoretical foundation for steering equivariant diffusion policies by proving that (i) the diffusion process of an EDP preserves the equivariance, resulting in an equivariant diffused marginal distribution, and (ii) the induced latent-noise MDP is group-invariant. This establishes when and why symmetry-preserving steering is possible. Next, we introduce a principled symmetry-aware steering framework that leverages these properties, enabling equivariant and approximately equivariant RL agents to exploit geometric structure during diffusion steering. Finally, through experiments on manipulation tasks with varying degrees of symmetry—including settings with extremely limited demonstrations—we show when strict equivariance yields the greatest benefit, when approximate equivariance is preferable under real-world symmetry breaking, and how symmetry-aware steering improves stability, prevents value divergence, and substantially enhances policy performance.

## 2. PRELIMINARIES

### 2.1 Diffusion Models

Denoising Diffusion Probabilistic Model (DDPM) (Ho et al., 2020) is a class of generative models that learn to approximate the data distribution  $q(a_0)$  by reversing a gradual noising process. Since we are interested in generating the desired action of a robot, we denote the data with the letter  $a$ .

**Forward Process.** The forward diffusion process is a Markov chain that incrementally adds Gaussian noise to a clean data sample  $a_0 \sim q(a_0)$  over  $T$  timesteps via a fixed variance schedule  $\{\beta_t\}$ . The transition kernel is defined as:

$$q(a_t|a_{t-1}) = \mathcal{N}(a_t; \sqrt{1 - \beta_t}a_{t-1}, \beta_t I).$$

We can sample  $a_t$  directly from  $a_0$ , using the diffusion kernel  $q(a_t|a_0) = \mathcal{N}(a_t; \sqrt{\bar{\alpha}_t}a_0, (1 - \bar{\alpha}_t)I)$ , where  $\alpha_t = 1 - \beta_t$  and  $\bar{\alpha}_t = \prod_{s=1}^t \alpha_s$ .

**Reverse Process.** The denoising process is defined as a reverse Markov chain that reconstructs the data distribution  $q(a_0)$  starting from a standard Gaussian prior  $p(a_T) = \mathcal{N}(0, I)$ . In practice, generation begins by sampling an initial latent noise  $w = a_T$  from this prior, which is then iteratively denoised to recover  $a_0$ . This reverse transition is approximated by a neural network parameterized by  $\theta$ :

$$p_\theta(a_{t-1}|a_t) = \mathcal{N}(a_{t-1}; \mu_\theta(a_t, t), \Sigma_\theta(a_t, t)).$$

The model is trained to predict the noise  $\epsilon$  added in the forward process by minimizing the simplified objective:

$$\mathcal{L} = \mathbb{E}_{t, a_0, \epsilon} [\|\epsilon - \epsilon_\theta(a_t, t)\|^2].$$

**Sampling via Langevin Dynamics.** Sampling is performed by iteratively refining the noise. The update rule at each step can be viewed as Langevin dynamics, utilizing the learned score function  $\nabla_{a_t} \log q(a_t) \propto -\epsilon_\theta(a_t, t)$  to guide samples toward high-density regions:

$$a_{t-1} = \frac{1}{\sqrt{\alpha_t}} \left( a_t - \frac{1 - \alpha_t}{\sqrt{1 - \bar{\alpha}_t}} \epsilon_\theta(a_t, t) \right) + \sigma_t z, \quad (1)$$

where  $z \sim \mathcal{N}(0, I)$  represents the stochastic noise injection, and  $\sigma_t$  controls the variance.

**Denoising Diffusion Implicit Models.** For inference, we employ Denoising Diffusion Implicit Model (DDIM) (Song et al., 2020). Its non-Markovian formulation allows for accelerated sampling with fewer denoising steps, effectively balancing computational efficiency and generation quality. Crucially, DDIM permits deterministic sampling ( $\sigma_t = 0$  in Eq. 1). Under this setting, a diffusion policy can be treated as a deterministic mapping  $\pi(s, w)$  from state  $s$  and latent noise  $w$  to action  $a$ .

### 2.2 Reinforcement Learning

We consider reinforcement learning in a Markov decision process (MDP)  $\mathcal{M} := (\mathcal{S}, \mathcal{A}, P, p_0, r, \gamma)$ , where  $\mathcal{S}$  denotes the state space,  $\mathcal{A}$  the action space,  $P$  the transition probability distribution,  $p_0$  the initial state distribution,  $r$  the reward, and  $\gamma$  the discount factor. The objective of reinforcement learning is to learn a policy  $\pi(a|s)$  that maximizes the expected discounted return  $\mathbb{E}[\sum_{t=0}^{\infty} \gamma^t r(s_t, a_t)]$ . Among many reinforcement learning algorithms, we highlight Soft Actor-Critic (SAC) (Haarnoja et al., 2018), a widely used off-policy actor-critic method.

### 2.3 Leveraging Group Symmetry

**Group Equivariance.** A function  $f : V_{\text{in}} \rightarrow V_{\text{out}}$  is equivariant to a group  $G$  if it commutes with group transformations. Formally, given group representations  $\rho_{\text{in}} : G \rightarrow \text{GL}(V_{\text{in}})$  and  $\rho_{\text{out}} : G \rightarrow \text{GL}(V_{\text{out}})$ ,  $f$  is equivariant if  $f(\rho_{\text{in}}(g)x) = \rho_{\text{out}}(g)f(x)$  for all  $g \in G, x \in V_{\text{in}}$ . For brevity, we denote this as  $f(gx) = gf(x)$ . In this work, we focus on the rotation group  $SO(2)$ , approximated by the cyclic subgroup  $C_N$ .

**Group-Invariant MDPs.** A  $G$ -invariant MDP  $\mathcal{M}_G$  (Wang et al., 2022a) is an MDP abstraction that reduces the original MDP model size (Ravindran and Barto, 2001, 2004). It satisfies two key conditions: 1) *Reward Invariance*:  $r(s, a) = r(gs, ga)$ , and 2) *Transition Invariance*:  $P(s'|s, a) = P(gs'|gs, ga)$ . In such MDPs, the optimal policy  $\pi^*$  is  $G$ -equivariant ( $\pi^*(gs) = g\pi^*(s)$ ) and the optimal critic  $Q^*$  is  $G$ -invariant ( $Q^*(gs, ga) = Q^*(s, a)$ ) (Wang et al., 2022a).

## 3. SYMMETRY IN DIFFUSION PROCESS

In this section, we derive mathematically that the diffusion process defined in equivariant diffusion policy and the diffused marginal distribution are equivariant. We note that the formulation of the equivariant diffusion process below is adapted from Ryu et al. (2024), tailored to the DDPM framework.

### 3.1 Symmetry in Task

We consider a robot manipulation task with inherent symmetry defined by a group  $G$ . We assume  $G$  is a group of transformations acting on state and action spaces, where each element  $g \in G$  is a volume-preserving transformation, i.e.  $|\det(J_g)| = 1$ , with  $J_g$  denoting the Jacobian matrix of  $g$ . The optimal policy for this task is described by a

target distribution  $q(a_0|s)$ , conditioned on the state  $s$ . We assume this distribution to be  $G$ -equivariant, satisfying  $q(ga_0|gs) = q(a_0|s)$ . Our goal is to approximate this with a diffusion model,  $p_\theta(a_0|s)$ .

### 3.2 Equivariant Diffusion Process

We begin by defining the property a diffusion kernel must satisfy to be compatible with the symmetry in task.

*Definition 1.* A diffusion kernel  $q(a_t|a_0)$  is defined as  $G$ -invariant if it satisfies the following condition for any group element  $g \in G$ :

$$q(ga_t|ga_0) = q(a_t|a_0).$$

*Remark 2.* The standard diffusion kernel is a  $G$ -invariant kernel for rotation groups. Its probability density is a function of the squared  $L_2$  norm  $\|a_t - \sqrt{\alpha_t}a_0\|^2$ , which is invariant under rotation transformations.

The following proposition proves that equivariance is preserved throughout the forward diffusion process, provided the process starts from an equivariant distribution.

*Proposition 3.* Let the clean action distribution  $q(a_0|s)$  be  $G$ -equivariant. If this distribution is perturbed by a  $G$ -invariant diffusion kernel  $q(a_t|a_0)$ , the resulting diffused marginal action distribution at step  $t$ ,

$$q(a_t|s) = \int q(a_0|s)q(a_t|a_0)da_0$$

is also  $G$ -equivariant, satisfying  $q(ga_t|gs) = q(a_t|s)$ .

**Proof.** For a transformed state  $gs$ , the diffused marginal distribution is:

$$q(ga_t|gs) = \int q(a'_0|gs)q(ga_t|a'_0)da'_0.$$

By the premise of  $G$ -equivariance for  $q(a_0|s)$ , we have  $q(a'_0|gs) = q(g^{-1}a'_0|s)$ . Performing a change of variables  $a_0 = g^{-1}a'_0$  (where  $da'_0 = da_0$  since  $G$  is volume-preserving), the integral becomes:

$$q(ga_t|gs) = \int q(a_0|s)q(ga_t|ga_0)da_0.$$

Since the kernel is  $G$ -invariant,  $q(ga_t|ga_0) = q(a_t|a_0)$ , this simplifies to:

$$q(ga_t|gs) = \int q(a_0|s)q(a_t|a_0)da_0 = q(a_t|s).$$

Thus, the diffused marginal distribution is  $G$ -equivariant.

Proposition 3 establishes that the forward diffusion process from a  $G$ -equivariant distribution results in a  $G$ -equivariant marginal distribution  $q(a_T|s)$ . While the denoising process is initialized from a prior distribution  $p(a_T)$ , effective generative modeling relies on the assumption that this prior closely approximates the diffused marginal  $q(a_T|s)$ . Consequently, to maintain consistency with the equivariant forward process, it is reasonable to assume the initial noise distribution used for equivariant denoising process to be  $G$ -equivariant. A standard equivariant diffusion policy, which leverages  $SO(2)$  symmetry and a corresponding invariant diffusion kernel (Remark 2), satisfies this by using an isotropic Gaussian prior  $\mathcal{N}(0, I)$ , which is naturally  $G$ -invariant for rotation groups. In contrast, a steering policy learns a state-dependent prior; thus, we assume that this learned distribution should satisfy  $G$ -equivariance.

## 4. SYMMETRY-PRESERVING STEERING WITH EQUIVARIANT REINFORCEMENT LEARNING

In this section, we formalize the steering problem within the latent-action MDP framework proposed by Wagenmaker et al. (2025) and show its group-invariance. The latent-action MDP defines the environment in which the reinforcement learning agent operates to steer the pre-trained diffusion policy. We further provide a theoretical justification for our method by demonstrating that an equivariant reinforcement learning agent can leverage symmetry when steering an equivariant diffusion policy.

### 4.1 Theory of Equivariant Diffusion Steering

Consistent with the task symmetry defined in Section 3.1, we define the underlying environment  $\mathcal{M}$  as a  $G$ -invariant MDP  $\mathcal{M}_G$  under the symmetry group  $G$ . We use a DDPM (Ho et al., 2020)-based policy during training but adopt the DDIM (Song et al., 2020) formulation for inference. Given a pre-trained equivariant diffusion policy  $\pi_{\text{edp}}$ , we define  $\pi_{\text{edp}}^{\mathcal{W}} : \mathcal{S} \times \mathcal{W} \rightarrow \mathcal{A}$  as the deterministic mapping which maps a state  $s \in \mathcal{S}$  and a latent noise  $w \in \mathcal{W}$  into an action  $a \in \mathcal{A}$ . We first state the equivariance with respect to the latent noise.

*Proposition 4.* The deterministic mapping  $\pi_{\text{edp}}^{\mathcal{W}}$  induced by an equivariant diffusion policy  $\pi_{\text{edp}}$  is equivariant with respect to the state and the initial latent noise, i.e.,  $\pi_{\text{edp}}^{\mathcal{W}}(gs, gw) = g\pi_{\text{edp}}^{\mathcal{W}}(s, w)$ .

**Proof.** Let  $\pi_{\text{edp}}^{\mathcal{W}}(s, w)$  denote the full denoising process of the equivariant diffusion policy, which maps a state  $s$  and an initial noise  $w = a_T$  to a final action. This process is defined by iteratively applying a one-step denoising function  $f_t$  for timesteps  $t = T, \dots, 1$ . Each step is defined as:

$$a_{t-1} = f_t(s, a_t) = \alpha_t(a_t - \gamma_t \epsilon_\theta(s, a_t, t))$$

where  $\epsilon_\theta$  is the noise prediction network and  $\alpha_t, \gamma_t$  are coefficients from the noise schedule.

The network  $\epsilon_\theta$  is equivariant by construction:

$$\epsilon_\theta(gs, ga_t, t) = g\epsilon_\theta(s, a_t, t)$$

Consequently, the one-step function  $f_t$  is also equivariant:

$$\begin{aligned} f_t(gs, ga_t) &= \alpha_t(ga_t - \gamma_t \epsilon_\theta(gs, ga_t, t)) \\ &= \alpha_t(ga_t - \gamma_t g\epsilon_\theta(s, a_t, t)) \\ &= g \cdot \alpha_t(a_t - \gamma_t \epsilon_\theta(s, a_t, t)) \\ &= g \cdot f_t(s, a_t) \end{aligned}$$

The full denoising process is a composition of these equivariant one-step functions:

$$\pi_{\text{edp}}^{\mathcal{W}}(s, w) = (f_1(s, \cdot) \circ f_2(s, \cdot) \circ \dots \circ f_T(s, \cdot))(w)$$

Since a composition of equivariant functions is itself equivariant, the entire policy  $\pi_{\text{edp}}^{\mathcal{W}}$  is equivariant with respect to the state and initial noise, which concludes the proof:

$$\pi_{\text{edp}}^{\mathcal{W}}(gs, gw) = g\pi_{\text{edp}}^{\mathcal{W}}(s, w)$$

The visualization of the equivariance in the latent-noise space is presented in Figure 1. Using Proposition 4, we now show that the latent-action MDP of an equivariant diffusion policy is  $G$ -invariant. With the mapping  $\pi_{\text{edp}}^{\mathcal{W}}$ , we can transform the action space  $\mathcal{A}$  of the MDP  $\mathcal{M}$  to

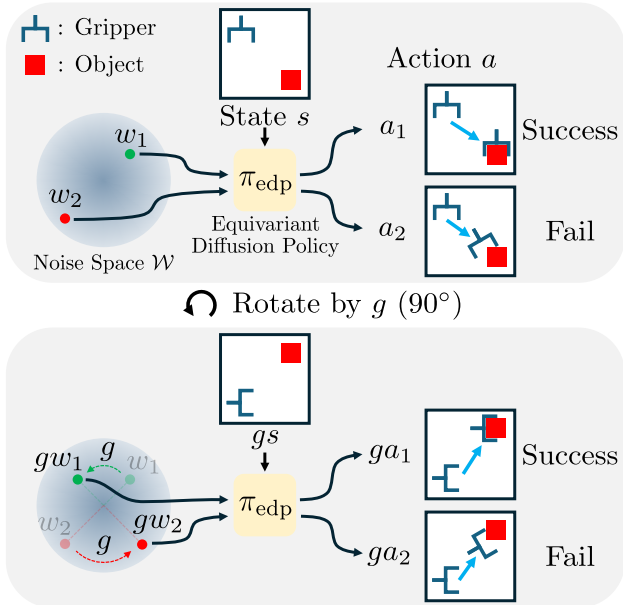


Fig. 1. **Equivariance in the latent-noise space.** The equivariant diffusion policy  $\pi_{\text{edp}}$  is equivariant with respect to the state  $s$  and the initial latent noise  $w$ . Consider an example task: grasping an object with a gripper. **Top:** The optimal latent noise  $w_1$  generates an optimal action  $a_1$ , while  $w_2$  leads to suboptimal action  $a_2$ . **Bottom:** When the state is transformed by  $g$  ( $90^\circ$ ), the transformed latent noises  $gw_1, gw_2$  lead to the transformed actions  $ga_1, ga_2$ . An equivariant steering policy trained to select  $w_1$  for  $s$  is structurally guaranteed to select the transformed noise  $gw_1$  for  $gs$ , which generates the optimal action  $ga_1$ .

a latent-noise space  $\mathcal{W}$ , thereby forming a latent-action MDP

$$\mathcal{M}^{\mathcal{W}} := (\mathcal{S}, \mathcal{W}, P^{\mathcal{W}}, p_0, r^{\mathcal{W}}, \gamma),$$

where

$$P^{\mathcal{W}}(\cdot | s, w) := P(\cdot | s, \pi_{\text{edp}}^{\mathcal{W}}(s, w)),$$

$$r^{\mathcal{W}}(s, w) := r(s, \pi_{\text{edp}}^{\mathcal{W}}(s, w)).$$

**Proposition 5.** The latent-action MDP,  $\mathcal{M}^{\mathcal{W}}$ , which is derived from a  $G$ -invariant MDP  $\mathcal{M}_G$  and an equivariant mapping  $\pi_{\text{edp}}^{\mathcal{W}}$ , is also a  $G$ -invariant MDP.

**Proof.** To prove that the latent-action MDP  $\mathcal{M}^{\mathcal{W}}$  is a  $G$ -invariant MDP, we must show that its reward and transition functions satisfy the two conditions of  $G$ -invariance.

1. *Reward Invariance.* By the definition of  $r^{\mathcal{W}}$ ,

$$r^{\mathcal{W}}(gs, gw) = r(gs, \pi_{\text{edp}}^{\mathcal{W}}(gs, gw)).$$

Applying Proposition 4, we obtain

$$r^{\mathcal{W}}(gs, gw) = r(gs, g\pi_{\text{edp}}^{\mathcal{W}}(s, w)).$$

Using the  $G$ -invariance of the original reward  $r$ , we have

$$r(gs, g\pi_{\text{edp}}^{\mathcal{W}}(s, w)) = r(s, \pi_{\text{edp}}^{\mathcal{W}}(s, w)),$$

which equals  $r^{\mathcal{W}}(s, w)$  by definition. Thus,

$$r^{\mathcal{W}}(gs, gw) = r^{\mathcal{W}}(s, w).$$

2. *Transition Invariance.* By the definition of  $P^{\mathcal{W}}$ ,

$$P^{\mathcal{W}}(gs' | gs, gw) = P(gs' | gs, \pi_{\text{edp}}^{\mathcal{W}}(gs, gw)).$$

Applying Proposition 4 again,

$$P^{\mathcal{W}}(gs' | gs, gw) = P(gs' | gs, g\pi_{\text{edp}}^{\mathcal{W}}(s, w)).$$

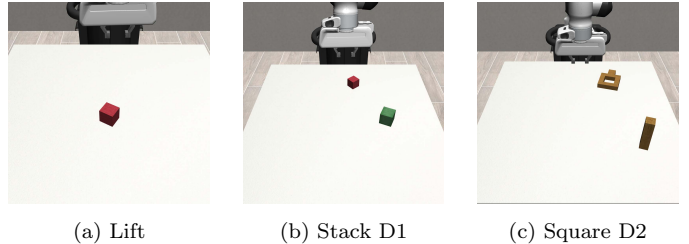


Fig. 2. **Task visualizations.** (a) **Lift:** Lifting a red cube. (b) **Stack D1:** Picking up a red cube (smaller) and stacking it onto a green cube (larger). (c) **Square D2:** Picking up a square nut and inserting it into a peg. Initial poses of the objects and the gripper are randomized in each episode.

Using the  $G$ -invariance of the transition kernel  $P$ , we obtain

$$P(gs' | gs, g\pi_{\text{edp}}^{\mathcal{W}}(s, w)) = P(s' | s, \pi_{\text{edp}}^{\mathcal{W}}(s, w)).$$

Therefore,

$$P^{\mathcal{W}}(gs' | gs, gw) = P^{\mathcal{W}}(s' | s, w).$$

Since both conditions are met, the latent-action MDP  $\mathcal{M}^{\mathcal{W}}$  is  $G$ -invariant.

Having established that the latent-action MDP is  $G$ -invariant, we now discuss the optimal strategy for steering.

#### 4.2 Equivariant Diffusion Steering with Equivariant SAC

Given that the latent-action MDP  $\mathcal{M}^{\mathcal{W}}$  is  $G$ -invariant, we leverage equivariant Soft Actor-Critic (SAC) (Haarnoja et al., 2018) to maximize the expected return. Specifically, we train a  $G$ -equivariant actor to learn the optimal steering policy, jointly with  $G$ -invariant critics that approximate the optimal action-value (Q) function. As established by Wang et al. (2022a), in a group-invariant MDP, the optimal Q-function is inherently  $G$ -invariant and the optimal policy is  $G$ -equivariant. This theoretical property justifies our architectural choice to enforce these geometric constraints, ensuring that the steering agent efficiently learns the optimal policy while respecting the underlying symmetry.

## 5. SIMULATION EXPERIMENTS

In this section, we present the simulation setup and empirical results with discussion. We conduct experiments on tasks from robotic manipulation benchmarks: **Robomimic** (Mandlekar et al., 2021) and **MimicGen** (Mandlekar et al., 2023), which provide manipulation tasks and expert demonstrations for imitation learning. The initial states of the tasks are visualized in Figure 2.

Our experiment consists of two stages. First, we pre-train a state-based variation of EDPs (Wang et al., 2024) on a given set of demonstrations. Second, we apply reinforcement learning on this pre-trained policy’s latent-noise space to “steer” the diffusion policy (Wagenmaker et al., 2025), in a direction of improving its performance through online interaction.

We mainly compare three steering methods:

- **(Standard) DSRL:** The baseline steering approach using a non-equivariant policy and critic, as proposed by Wagenmaker et al. (2025).
- **Equi-DSRL:** Our proposed method, which employs a  $G$ -equivariant steering policy and  $G$ -invariant critics designed to follow the system’s underlying symmetries.
- **Approx-Equi-DSRL:** A variant of our proposed method, which employs approximately  $G$ -equivariant steering policy and approximately  $G$ -invariant critics. In this work, we implemented this variant following the mechanism of Finzi et al. (2021).

For all experiments, we report the mean success rate and standard error averaged over five random seeds. Evaluations are performed periodically during training, each consisting of 50 episodes. We also assess training stability by monitoring the mean  $Q$ -values of sampled transitions. The results are visualized in Figure 3, and the peak success rates achieved during training are detailed in Table 1.

### 5.1 Implementation Details

Unless otherwise specified, all experiments share the following setup.

**Base Equivariant Diffusion Policy.** We adapt the  $SO(2)$ -equivariant framework of Wang et al. (2024) to a state-based setting. The observation  $s$  includes proprioceptive and object states, while the action  $a$  consists of absolute gripper poses and widths for the next 4 timesteps (see Appendix A for representation details). Instead of the original U-Net, we employ a  $C_8$ -equivariant MLP backbone constructed with `escnn` linear layers (Cesa et al., 2022), aligning with the prior work (Wagenmaker et al., 2025). Training utilizes the DDPM objective (Ho et al., 2020) with 100 steps, while inference employs deterministic DDIM sampling (Song et al., 2020) with 5 steps.

**Steering Algorithm.** We utilize the DSRL-SAC algorithm (Wagenmaker et al., 2025) operating in the latent-noise space  $\mathcal{W}$ . To ensure a fair comparison, all actor and critic networks use 3-layer MLPs with dimensions adjusted to match the total parameter count. Specifically, the non-equivariant DSRL baseline uses 2048 hidden units per layer, whereas Equi-DSRL uses 768 hidden units with  $C_8$  regular representations. For Approx-Equi-DSRL, we adopt a hybrid architecture that sums outputs from parallel equivariant and non-equivariant layers (256 hidden units each). Leveraging the soft equivariance strategy proposed in Finzi et al. (2021), we apply different weight decays:  $10^{-5}$  for the equivariant layers and  $10^{-2}$  for the non-equivariant layers. The other hyperparameters follow Wagenmaker et al. (2025).

### 5.2 Steering in the Low-Data Regime

**Experimental Setup.** We first investigate a scenario defined by extreme data scarcity. We use the Lift task from Robomimic, a task with relatively low difficulty. The base EDP is pre-trained on an extremely limited expert dataset of only three (3) demonstrations. This setup creates a challenging testbed where the base policy has a low capability, requiring effective and efficient online improvement.

Table 1. Maximum evaluation success rates.

Task	Before Steering	DSRL	Equi-DSRL	Approx-Equi-DSRL
Lift	0.617	0.808	<b>0.840</b>	0.820
Stack D1	0.568	0.740	0.728	<b>0.800</b>
Square D2	0.275	0.552	<b>0.644</b>	0.604

**Results.** As visualized in Figure 3 and quantified in Table 1, both equivariant and approximately equivariant steering strategies proved highly effective, significantly outperforming the base policy. Equi-DSRL achieved the highest peak success rate, closely followed by Approx-Equi-DSRL. In contrast, standard DSRL exhibited severe instability; despite showing initial improvement, it frequently (3 out of 5 seeds) suffered from performance collapse attributed to significant  $Q$ -value divergence.

### 5.3 Steering for Complex Tasks

**Experimental Setup.** We evaluate performance on a more complex manipulation task to assess sample efficiency under more typical training conditions. We use the Stack D1 and Square D2 tasks from MimicGen, which involve a broader initial state distribution and require greater precision. For this experiment, the base EDPs are pre-trained on 100 and 200 demonstrations, respectively.

**Results.** As illustrated in Figure 3 and quantified in Table 1, Approx-Equi-DSRL demonstrated the most robust performance across complex tasks. In Stack D1, it achieved the highest efficacy, while Equi-DSRL exhibited the lowest overall performance. However, in Square D2, both Equi-DSRL and Approx-Equi-DSRL reached comparable superior performance. A consistent pattern observed in standard DSRL across both tasks was initial training instability; it suffered from early  $Q$ -value divergence and performance degradation. While it eventually recovered, it remained the lowest-performing method in Square D2 and failed to match the best strategy in Stack D1.

### 5.4 Discussion

Our experimental results reveal some aspects of integrating equivariance into the steering process.

**Task-Dependent Benefits of Equivariance.** We observe that the sample efficiency gains from Equi-DSRL and Approx-Equi-DSRL are more pronounced in complex tasks compared to a relatively simple task. We attribute this discrepancy to the varying advantage of equivariance, which correlates with the extent to which the task demands spatial generalization. In the Lift task, which simply involves picking up an object confined to a small range, the exploitation of rotational symmetry is less critical. Conversely, Stack D1 and Square D2 require more complex manipulation involving significant rotational variations, with objects initialized over a much wider  $xy$ -area. This combination of complex manipulation and expanded workspace utilization makes the rotational symmetry of the task more important, corresponding to a higher level of equivariance (Wang et al., 2024). Our results confirm that equivariant steering yields superior sample efficiency when the task’s spatial configuration actively engages these symmetries.

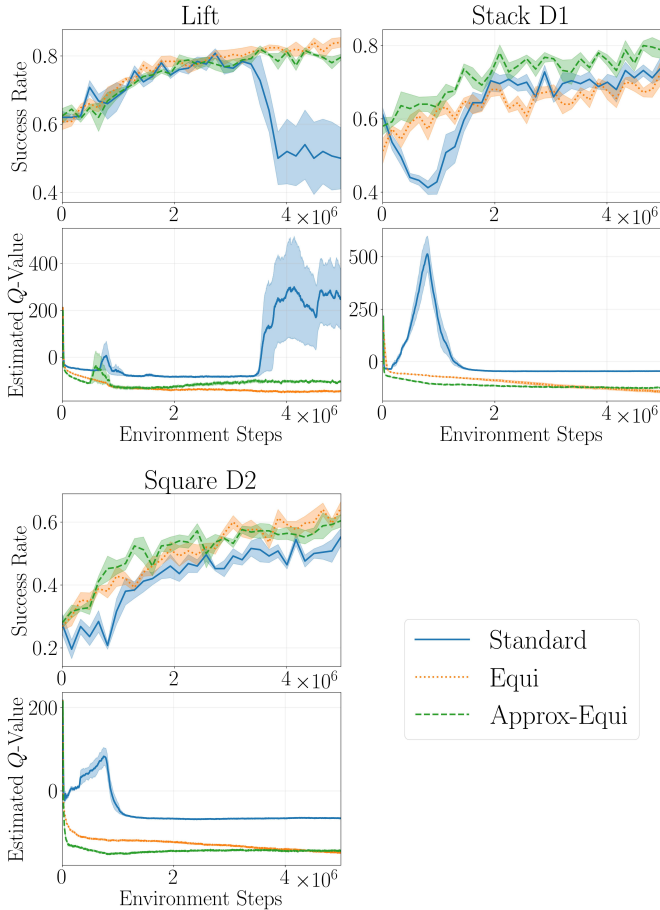


Fig. 3. **Performance comparison.** Results are averaged over 5M environment steps, using five random seeds. Shaded regions denote standard error.

**Impact of Symmetry Breaking.** In the Stack D1 task, Equi-DSRL exhibited lower final performance compared to the standard DSRL, despite its theoretical efficiency. We attribute this degradation to symmetry breaking inherent in realistic robotic manipulation, specifically caused by joint limits and kinematic singularities. The Stack D1 task is particularly susceptible to this issue due to its requirement for a wide range of gripper movements compared to the Lift task. Consequently, the strict symmetry enforcement in Equi-DSRL becomes a liability. This finding underscores the advantage of Approx-Equi-DSRL, which relaxes these strict constraints to adapt to environmental asymmetries, thereby achieving superior performance.

**Preventing Instability from High Update Ratios.** While high update-to-data (UTD) ratios are presented as a best practice for DSRL (Wagenmaker et al., 2025), such regimes are prone to  $Q$ -value divergence in off-policy actor-critic methods (Hussing et al., 2025). We empirically observed this instability in our non-equivariant baseline; specifically, during the early stages of Stack D1 and Square D2, and the later stages in a subset of Lift trials (3 out of 5 seeds), the critic exhibited severe  $Q$ -value divergence. This divergence led the steering policy towards suboptimal regions of the latent-noise space, resulting in performance collapse. We attribute this instability to the overestimation of out-of-distribution (OOD) actions (Hussing et al., 2025), which can be effectively prevented

in our equivariant DSRL. By enforcing the constraint  $Q(s, a) = Q(gs, ga) \forall g \in G$ , the group-invariant critic implicitly treats a single transition as a learning signal for all symmetrically equivalent states. This structural prior effectively reduces the size of the solution space (Van der Pol et al., 2020), inherently shrinking the set of OOD actions. We find that this reduction suppresses the overestimation of  $Q$ -value estimates, thereby preventing the divergence common in high-UTD learning. Consequently, equivariant DSRL estimates more conservative and realistic  $Q$ -values, steering the policy more reliably.

## 6. CONCLUSION AND FUTURE WORK

In this work, we proposed equivariant DSRL framework, a theoretically grounded approach for steering equivariant diffusion policies. We demonstrated that this approach enables effective improvement even from base policies trained with limited demonstrations. Through a comparative analysis of standard, equivariant, and approximately equivariant strategies, we provided practical guidelines for diverse settings. Future work could extend this by applying equivariance priors to steer non-equivariant policies.

### DECLARATION OF GENERATIVE AI AND AI-ASSISTED TECHNOLOGIES IN THE WRITING PROCESS

During the preparation of this work the authors used Gemini in order to generate code snippets and polish texts. After using this tool, the authors reviewed and edited the content as needed and take full responsibility for the content of the publication.

## REFERENCES

- Cesa, G., Lang, L., and Weiler, M. (2022). A program to build  $E(N)$ -equivariant steerable CNNs. In *International Conference on Learning Representations (ICLR)*.
- Chang, J., Park, M., Seo, J., Horowitz, R., Lee, J., and Choi, J. (2025). Partially equivariant reinforcement learning in symmetry-breaking environments. *arXiv preprint arXiv:2512.00915*.
- Chi, C., Feng, S., Du, Y., Xu, Z., Cousineau, E., Burchfiel, B., and Song, S. (2023). Diffusion policy: Visuomotor policy learning via action diffusion. In *Proceedings of Robotics: Science and Systems (RSS)*.
- Finzi, M., Benton, G., and Wilson, A.G. (2021). Residual pathway priors for soft equivariance constraints. In *Advances in Neural Information Processing Systems*, volume 34.
- Haarnoja, T., Zhou, A., Abbeel, P., and Levine, S. (2018). Soft actor-critic: Off-policy maximum entropy deep reinforcement learning with a stochastic actor. In *International conference on machine learning*, 1861–1870. Pmlr.
- Ho, J., Jain, A., and Abbeel, P. (2020). Denoising diffusion probabilistic models. *Advances in neural information processing systems*, 33, 6840–6851.
- Hussing, M., Voelcker, C.A., Gilitschenski, I., Farahmand, A.m., and Eaton, E. (2025). Dissecting deep RL with high update ratios: Combatting value divergence. *Reinforcement Learning Journal*, 2, 995–1018.

Mandlekar, A., Nasiriany, S., Wen, B., Akinola, I., Narang, Y., Fan, L., Zhu, Y., and Fox, D. (2023). Mimicgen: A data generation system for scalable robot learning using human demonstrations. *arXiv preprint arXiv:2310.17596*.

Mandlekar, A., Xu, D., Wong, J., Nasiriany, S., Wang, C., Kulkarni, R., Fei-Fei, L., Savarese, S., Zhu, Y., and Martín-Martín, R. (2021). What matters in learning from offline human demonstrations for robot manipulation. *arXiv preprint arXiv:2108.03298*.

Ravindran, B. and Barto, A.G. (2001). Symmetries and model minimization in markov decision processes.

Ravindran, B. and Barto, A.G. (2004). Approximate homomorphisms: A framework for non-exact minimization in markov decision processes.

Ren, A.Z., Lidard, J., Ankile, L.L., Simeonov, A., Agrawal, P., Majumdar, A., Burchfiel, B., Dai, H., and Simchowitz, M. (2024). Diffusion policy optimization. *arXiv preprint arXiv:2409.00588*.

Ryu, H., Kim, J., An, H., Chang, J., Seo, J., Kim, T., Kim, Y., Hwang, C., Choi, J., and Horowitz, R. (2024). Diffusion-edfs: Bi-equivariant denoising generative modeling on se (3) for visual robotic manipulation. In *Proceedings of the IEEE/CVF Conference on Computer Vision and Pattern Recognition*, 18007–18018.

Ryu, H., Lee, H.i., Lee, J.H., and Choi, J. (2023). Equivariant descriptor fields: SE(3)-equivariant energy-based models for end-to-end visual robotic manipulation learning. *International conference on learning representations (ICLR)*.

Seo, J., Kruthiventy, A., Lee, S., Teng, M., Zhang, X., Choi, S., Choi, J., and Horowitz, R. (2025a). Equicontact: A hierarchical se (3) vision-to-force equivariant policy for spatially generalizable contact-rich tasks. *arXiv preprint arXiv:2507.10961*.

Seo, J., Prakash, N.P., Zhang, X., Wang, C., Choi, J., Tomizuka, M., and Horowitz, R. (2023). Contact-rich se (3)-equivariant robot manipulation task learning via geometric impedance control. *IEEE Robotics and Automation Letters*, 9(2), 1508–1515.

Seo, J., Yoo, S., Chang, J., An, H., Ryu, H., Lee, S., Kruthiventy, A., Choi, J., and Horowitz, R. (2025b). Se (3)-equivariant robot learning and control: A tutorial survey. *International Journal of Control, Automation and Systems*, 23(5), 1271–1306.

Song, J., Meng, C., and Ermon, S. (2020). Denoising diffusion implicit models. *arXiv preprint arXiv:2010.02502*.

Van der Pol, E., Worrall, D., van Hoof, H., Oliehoek, F., and Welling, M. (2020). Mdp homomorphic networks: Group symmetries in reinforcement learning. *Advances in Neural Information Processing Systems*, 33, 4199–4210.

Wagenmaker, A., Nakamoto, M., Zhang, Y., Park, S., Yagoub, W., Nagabandi, A., Gupta, A., and Levine, S. (2025). Steering your diffusion policy with latent space reinforcement learning. *Conference on Robot Learning (CoRL)*.

Wang, D., Hart, S., Surovik, D., Kelestemur, T., Huang, H., Zhao, H., Yeatman, M., Wang, J., Walters, R., and Platt, R. (2024). Equivariant diffusion policy. In *8th Annual Conference on Robot Learning*. URL <https://openreview.net/forum?id=wD2kUVLT1g>.

Wang, D., Walters, R., and Platt, R. (2022a). SO(2)-equivariant reinforcement learning. In *International Conference on Learning Representations*. URL <https://openreview.net/forum?id=7F9c0hdvfk>.

Wang, R., Walters, R., and Yu, R. (2022b). Approximately equivariant networks for imperfectly symmetric dynamics. In *International Conference on Machine Learning*, 23078–23091. PMLR.

## Appendix A. STATE AND ACTION SPACE REPRESENTATIONS OF THE TASKS

We use two kinds of group representations: (i) trivial representation  $\rho_0$  which acts on an invariant scalar  $x \in \mathbb{R}$  by  $\rho_0(g)x = x$ , (ii) irreducible representation (Irrep)  $\rho_w$  of the group  $SO(2)$  or  $C_N$  which acts on a vector  $x \in \mathbb{R}^2$  by a rotation of frequency  $w$ ,  $\rho_w(g)x = \begin{bmatrix} \cos wg & -\sin wg \\ \sin wg & \cos wg \end{bmatrix} x$ .

Details of state and action representations are specified in Tables A.1–A.4. The symbol  $\oplus$  denotes direct sum, and the notation  $\rho^n$  indicates the  $n$ -fold direct sum of the representation  $\rho$ .

Table A.1. Lift state representations

Name	Dim	Rep
cube position $(x, y, z)$	3	$\rho_1 \oplus \rho_0$
cube 6d rotation	6	$\rho_1^3$
gripper to cube position $(x, y)$	2	$\rho_1$
gripper position $(x, y, z)$	3	$\rho_1 \oplus \rho_0$
gripper 6d rotation	6	$\rho_1^2$
gripper joint position	2	$\rho_0^2$

Table A.2. Stack D1 state representations

Name	Dim	Rep
cube position $(x, y, z)$	3	$\rho_1 \oplus \rho_0$
cube 6d rotation	6	$\rho_1^3$
gripper to cube position $(x, y, z)$	3	$\rho_1 \oplus \rho_0$
gripper position $(x, y, z)$	3	$\rho_1 \oplus \rho_0$
gripper 6d rotation	6	$\rho_1^3$
gripper joint position	2	$\rho_0^2$

Table A.3. Square D2 state representations

Name	Dim	Rep
nut position $(x, y, z)$	3	$\rho_1 \oplus \rho_0$
nut 6d rotation	6	$\rho_1^3$
gripper to nut position $(x, y, z)$	3	$\rho_0^3$
gripper to nut 6d rotation	6	$\rho_0^6$
peg position $(x, y, z)$	3	$\rho_1 \oplus \rho_0$
gripper position $(x, y, z)$	3	$\rho_1 \oplus \rho_0$
gripper 6d rotation	6	$\rho_1^3$
gripper joint position	2	$\rho_0^2$

Table A.4. Action representations

Name	Dim	Rep
gripper position $(x, y, z)$	3	$\rho_1 \oplus \rho_0$
gripper 6d rotation	6	$\rho_1^3$
gripper width	1	$\rho_0$